Available online at www.sciencedirect.com
ScienceDirect
Trans. Nonferrous Met. Soc. China 20(2010) 259−266
Transactions of Nonferrous Metals Society of China
www.tnmsc.cn

Die structure optimization of equal channel angular extrusion for AZ31 magnesium alloy based on finite element method

HU Hong-jun(胡红军)[1, 2], ZHANG Ding-fei(张丁非)[1, 3], PAN Fu-sheng(潘复生)[1, 3]

1. National Engineering Research Center for Magnesium Alloys, Chongqing University, Chongqing 400044, China;
2. College of Materials Science and Engineering, Chongqing University, Chongqing 400045, China;
3. College of Materials Science and Engineering, Chongqing Institute of Technology, Chongqing 400050, China

Received 4 November 2008; accepted 4 February 2009

Abstract: Three-dimensional(3D) geometric models with different corner angles (90° and 120°) and with or without inner round fillets in the bottom die were designed. Some important process parameters were regarded as the calculation conditions used in DEFORM^{TM}-3D software, such as stress—strain data of compression test for AZ31 magnesium, temperatures of die and billet, and friction coefficient. Influence of friction coefficient on deformation process was discussed. The results show that reasonable lubrication condition is important to plastic deformation. The change characteristics for distributions of effective stress and strain during an equal channel angular extrusion (ECAE) process with inner angle of 90° and without fillets at outer corner were described. Inhomogeneity index (C) was defined and deformation heterogeneity of ECAE was analyzed from the simulation and experiment results. The deformation homogeneity caused by fillets at outer corner increased compared with the die without fillets. The cumulated maximum strains decrease with increasing the fillets of outer corner in ECAE die and the inner corner angle. The analysis results show that better structures of ECAE die including appropriate outer corner fillet and the inner corner angle of 90° for the die can improve the strain and ensure plastic deformation homogenization to a certain extent. The required extrusion force drops with increasing the fillet made at outer corner in ECAE die. It is demonstrated that the prediction results are in good agreement with experiments and the theoretical calculation and the research conclusions in literatures.

Key words: AZ31 magnesium alloy; equal channel angular extrusion; finite element method; outer corner angle; deformation inhomogeneity

1 Introduction

Finite element method (FEM) is one of the important approaches to understand the deformation occurring in the equal channel anglar extrusion (ECAE) process. Many FEM-based analyses have been performed to determine the deformation behavior of materials and to estimate the developed strain in the ECAP process[1−3]. However, the past studies assumed 2D approximation of plane strain condition and did not discuss the inhomogeneity of stress and strain. Results obtained by 2D analysis give limited information, in addition to the inherent 2D approximation errors[4−8]. But few researchers adopted 3D simulation technologies to investigate the deformation behaviors of magnesium AZ31, especially the influence of die structure on strain distribution and extrusion quality. Many of the early studies on ECAP were limited to the processing of soft pure metals or solid solution alloys. Much recently, significant attention has been devoted to the pressing of more complex alloys and fairly hard metals with limited numbers of slip systems, especially for magnesium alloys. For these difficult-to-work materials, three different strategies have been adopted with the overall objective of achieving successful processing by ECAE[9−11]. Current research interest is in the processing to obtain fine-grained bulk magnesium alloy specimens by ECAE. The numerical simulation with the help of the finite element method (FEM) has been extensively used to better understand the ECAE method [12−15].

In the present work, a quasi-static solution to the ECAE method by the FEM simulations was carried out

Foundation item: Project(2007CB613700) supported by National Basic Research Program of China; Project(2006BAE04B03) supported by Item of Support Plan during the 11th National Five-Year Plan; Projects(CST, 2007bb4413) supported by National Science Foundation of Chongqing, China

Corresponding author: HU Hong-jun; Tel: +86-23-68851783; Fax: +86-23-68851783; E-mail: hhj@cqit.edu.cn

DOI: 10.1016/S1003-6326(09)60132-1

using dies with intersecting angles of 90° and 120°, considering only one pass of extrusion. This study is to numerically analyze the deformation behaviors in ECAE of AZ31 magnesium alloy and predict the strain, stress and extrusion force of ECAE to form nanostructure processed based on various die structures.

2 Simulation and experiment

The sketch map of a tool is depicted in Fig.1. The bottom die consists of two intersecting channels with the same cross section meeting at an inner corner angle Φ (see Fig.1). In this work, the use of the extreme principle, for instance, the upper bound method, has gained a lot of attention to estimate the pressure needed for the plunger as well as the accumulated effective strain resulting from the ECAE method.

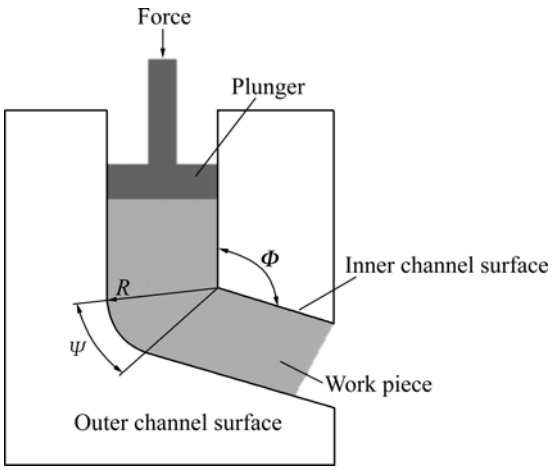

Fig.1 Sketch map of tool (Inner corner angle Φ, and outer corner angle ψ)

The billet made of AZ31 (Mg-3%Al-1%Zn, mass fraction) is assumed to be elastoplastic material. Physical properties of the AZ31 workpiece are listed in Table 1 [16−20]. The following assumptions were adopted in the present analyses: 1) both the container and the die are rigid bodies; 2) the extrusion billet is a rigid-plastic material[21−23]; and 3) the friction coefficient between the extrusion billet and the ram, container, and die is constant.

Table 1 Physical properties of AZ31 alloy

Poisson ratio	Coefficient of linear expansion/K^{-1}	Density/ ($kg \cdot m^{-3}$)	Elastic modulus/ MPa	Emissivity
0.35	2.68×10^{-5}	1 780	45 000	0.12

Four distinct geometric models for the ECAE die have been developed. The channel intersection angles, Φ=90° and Φ=120° are considered and illustrated in Fig.2(a) and Fig.2(b). The modified geometric models with inner round fillets are illustrated in Fig.2(c) and Fig.2(d). The geometrical parameters of the ECAE dies in Fig.2 are listed in Table 2. The material of ECAE dies is H13 hot-work tool steel. Simulation and experimental parameters including dimensions of billet and die are listed in Table 3.

The flow stress—strain data of the AZ31 alloy were determined through hot compression tests using Gleeble1500D machine in Laboratory of National Engineering Research Center for Magnesium Alloys in China. The flow stress curves measured in these tests were corrected and a set of flow stress—strain curves are shown in Fig.3. The data over a temperature range of 300−500 ℃ and a strain rate range of 0.01−10 s^{-1} were input into the DEFORM^{TM}-3D.

Extrusion experiments were carried out to verify the results obtained from computer simulation in the laboratory. In order to validate the results of finite element analysis, the ECAE dies of inner angle 90° without fillets and with fillets at outer corner were designed and manufactured to perform the actual extrusion processes. Before extrusion the billets were machined into rods with diameter of 16 mm. Real extrusion experiments were carried out employing a press of 98 kN with a resistance heated container and a heater. Die material, die dimensions, billet dimensions and extrusion conditions were all the same as those used in numerical simulation as described above. The billet was heated in an external furnace up to 300 ℃ and transported into the container at a preset temperature of 275 ℃ to avoid too much heat dissipation and then extrusion started immediately. Ram speed was 5 mm/s during experimental verification. Extrusion pressure was measured by a pressure sensor and ram time. After the extrusion cycle, the evolutions of extrusion force during extrusion were plotted against extrusion strokes.

The friction at workpiece/tooling interface was assumed to be of shear type. The friction coefficient f ($0<f<1$) is expressed as[24−25]

$$f=\sqrt{3}\frac{\tau}{\sigma} \tag{1}$$

where τ is the frictional shear stress and σ the effective flow stress of the billet material. In the present simulation, a friction coefficient of 0.25 was assumed to be at the billet-container and billet-stem interfaces. And the friction coefficient at the die/extrudate interface was chosen to be 0.25 too.

3 Results and discussion

3.1 Influence of friction coefficient on deformation process

In any metal forming process, the surfaces of the die

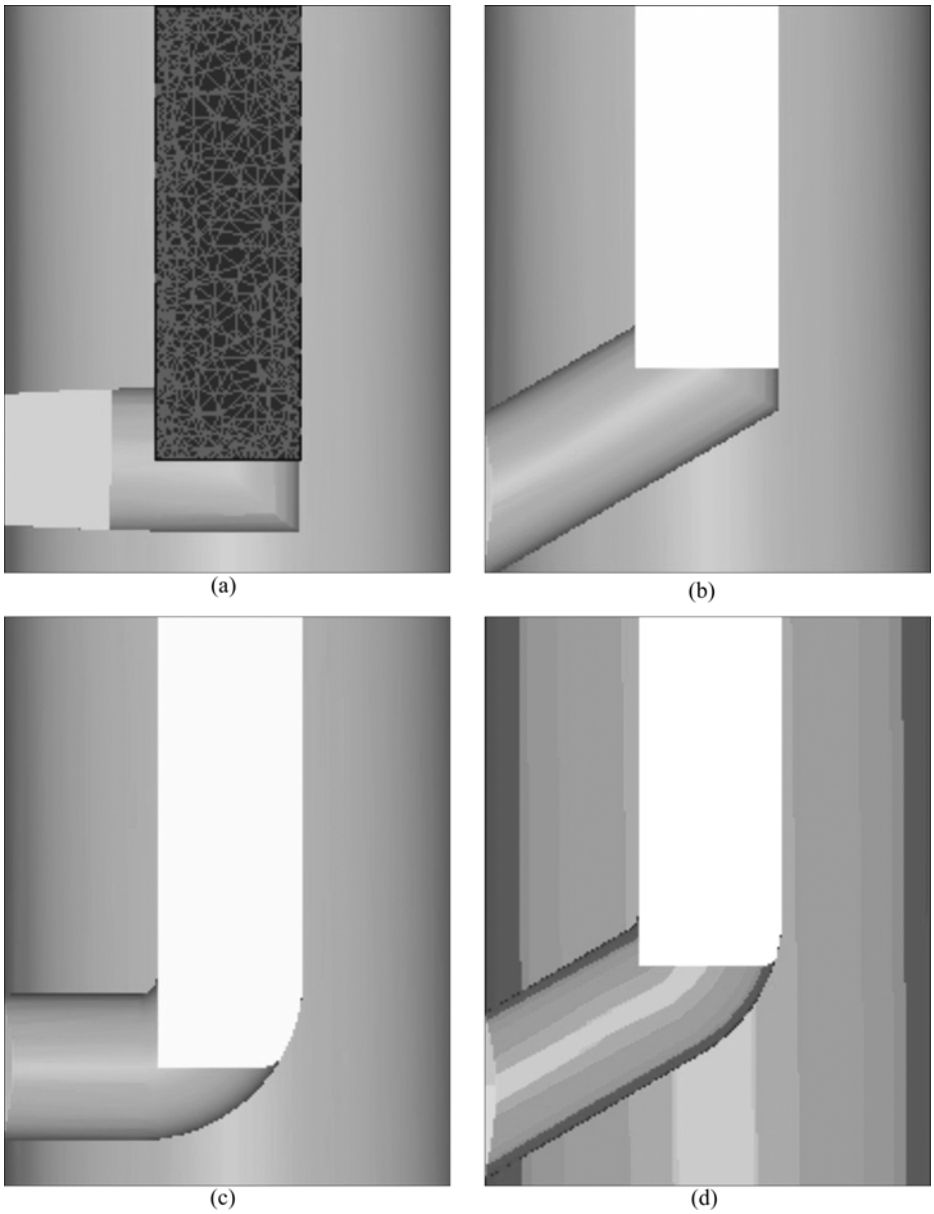

Fig.2 Geometric models of dies with different inner corner angles and without or with fillets: (a) 90˚, without fillets; (b) 120˚, without fillets; (c) 90˚, with fillets; (d) 120˚, with fillets

Table 2 Geometrical parameters of ECAE die

Location	Φ/(˚)	Ψ/(˚)	R/mm	r/mm
Fig.2(a)	90	0	0	0
Fig.2(b)	120	0	18	2
Fig.2(c)	90	90	0	0
Fig.2(d)	120	60	18	2

and the workpiece are never perfectly smooth. When no lubrication is provided, contact between the asperities of both surfaces is maintained. The asperities of the workpiece provide an area of contact large enough to support the total average pressure required for the process. The actual contact area between the flattened asperities of the workpiece and the die is smaller than the apparent total area. When lubrication is provided, some lubricant is dragged between the two surfaces by moving the workpiece. As velocity or liquid viscosity increases, the more the voids between the surfaces are filled with lubricant, the more the pressure on the workpiece is transferred through the lubricant and the less the load acts to smooth down the asperities of the workpiece. There is less actual metal-to-metal contact, so friction drops. The friction coefficient can indicate the lubrication conditions. The friction coefficient of 0.1, 0.25 and 0.5 were chosen in the simulations respectively.

Figs.4(a)−(d) shows the influence of friction coefficient on deformation process including extrusion force, the maximum strain, the maximum velocity and the maximum stress.

Table 3 Simulation and experimental parameters

Billet length/ mm	Billet diameter/ mm	Inside diameter of ECAE die/mm	Outside diameter of die/mm	Initial billet temperature/ ℃
50	16	16	50	300
Initial tooling temperature/℃	Temperature range for flow stress measurement/℃	Ram speed/(mm·s^{-1})	Friction coefficient of container/billet interface	Friction coefficient between billet and die
275	250−450	10	0.25	0.25
Total number of elements of billet	Total number of elements of plunger	Total number of elements of die	Mesh density type	Relative interference depth
20 000	8 000	20 000	Relative	0.7

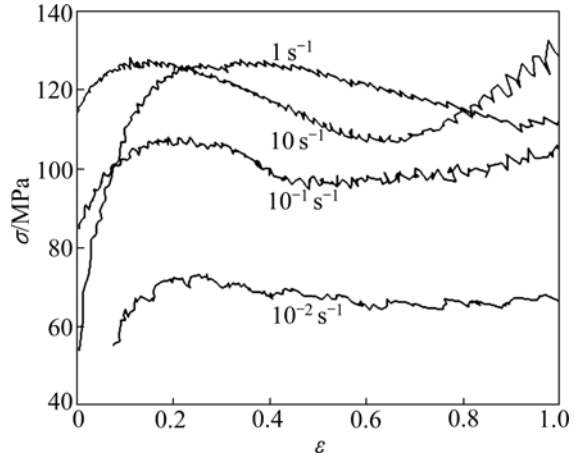

Fig.3 Curves of stress—strain of AZ31 at 300 ℃ under different strain rates

From Fig.4(a) the influence of friction coefficient on the requirement of the extrusion force is very obvious. With increasing the friction coefficient, the required maximum extrusion force increases and the time when the extrusion force reaches the summit is delayed. If the friction coefficient is equal to 0.5, the fluctuation of extrusion force is wider than that caused by friction coefficient of 0.10 or 0.25. From Fig.4(b), the influence of friction coefficient on the maximum strain is very obvious. With increasing the friction coefficient, the maximum strain increases. The variation trends of the maximum strain with friction coefficient are approximate. From Fig.4(c), the influence of friction coefficient on the maximum velocity is very obvious. It can be concluded that the maximum flow velocity of metal during extrusion process is decreased with increasing friction coefficient. From Fig.4(d), it is discovered that the maximum effective stress has little change during former extrusion period; but later variation trend is adverse; smaller friction coefficient would cause larger stress fluctuation in the extrusion rod.

3.2 Distribution of effective stress and strain during ECAE process

Fig.5 shows the distribution and development of the equivalent stress and strain of step 40 and step 90 of the ECAE die with inner angle 90° and without fillets at outer corner. The effective stresses of the material are not even seen from Fig.5(a) and Fig.5(c), the effective stress of about 117 MPa is the largest at the corner near the wall of the bottom die at step 90. The deformation of the initial extrusion is nonuniform, and the largest strain from Fig.5(b) appears at outer corner in the step 40. Distributions of the strain are lamellar with distinct deformation gradients at the corner. This shows that the deformation of this position is near to the simple shear deformation. But deformation heterogeneity becomes better in step 90 from Fig.5(d) than in step 40 from Fig.4(b).

3.3 Comparison of strain under different conditions from simulation, theory and experiment

3.3.1 Analysis of deformation homogeneity for ECAE products

Fig.6 shows the distributions of the equivalent strains at extrusion step 40 and 90 caused by ECAE die with outer corner angle of 90° and fillets at the outer corner. It can be clearly found that the deformation homogeneity in Figs.6(a) and (b) is increased compared with the contours in Figs.5(b) and (d); at the same time the effective strain decreases. The shape of billet in Fig.6(b) is less damaged than that in Fig.5(d). To quantify the degree of deformation inhomogeneity, a deformation inhomogeneity index (C) is defined as follows:

$$C = \frac{\varepsilon_{\max} - \varepsilon_{\min}}{\varepsilon_{\text{ave}}} \tag{2}$$

where $\varepsilon_{\max}$, $\varepsilon_{\min}$ and ε_{ave} denote the maximum, minimum and average of equivalent plastic strains, respectively. The effective strain and deformation inhomogeneity indexes under different conditions of extrusion step 90 are listed in Table 4. It is found that the effective strains (including $\varepsilon_{\max}$, $\varepsilon_{\min}$ and ε_{ave}) decrease with increasing inner corner angle and fillets at outer corner. The deformation inhomogeneity indexs vary with the inner corner angle and with fillets or not. This shows that the homogeneity caused by ECAE die with inner corner

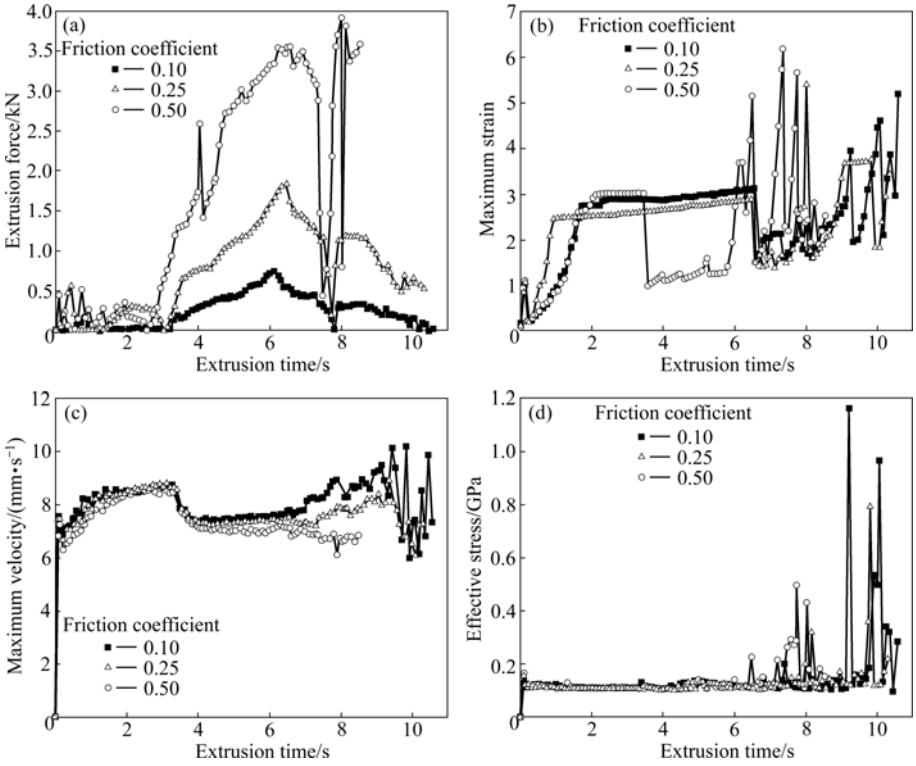

Fig.4 Influence of friction coefficient on deformation process: (a) Extrusion force vs extrusion time; (b) Maximum extrusion strain vs extrusion time; (c) Maximum extrusion velocity vs extrusion time; (d) Maximum effective extrusion stress vs extrusion time

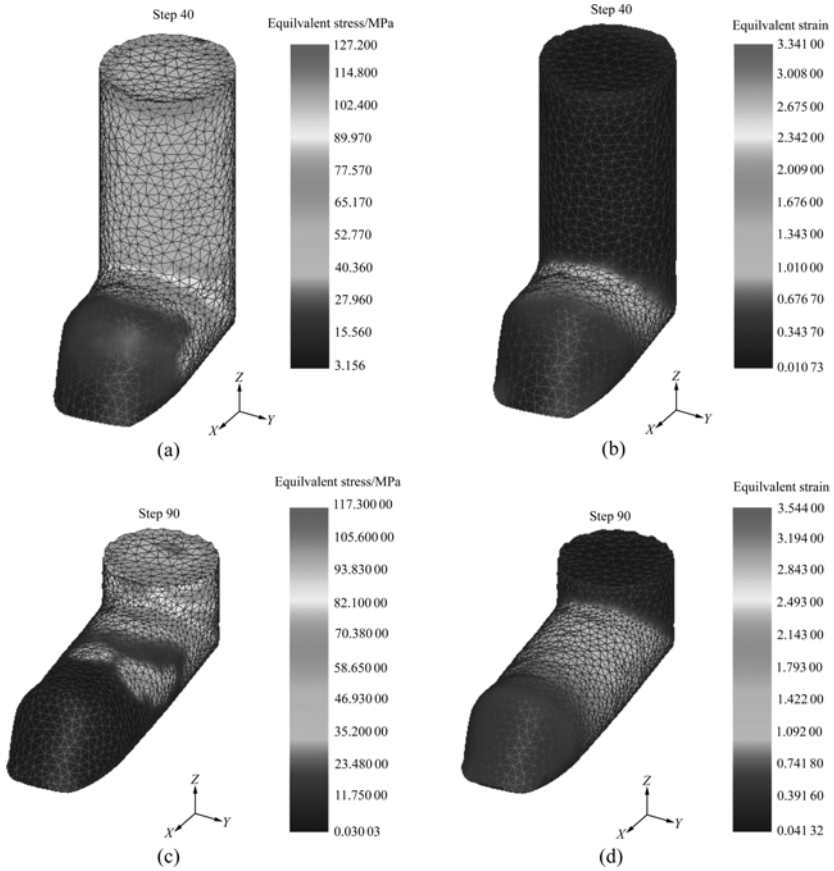

Fig.5 Distributions of equivalent stress and strain with angle 90˚ and without outer corner fillets: (a) Contours of effective stress of step 40; (b) Contours of effective strain of step 40; (c) Contours of effective stress of step 90; (d) Contours of effective strain of step 90

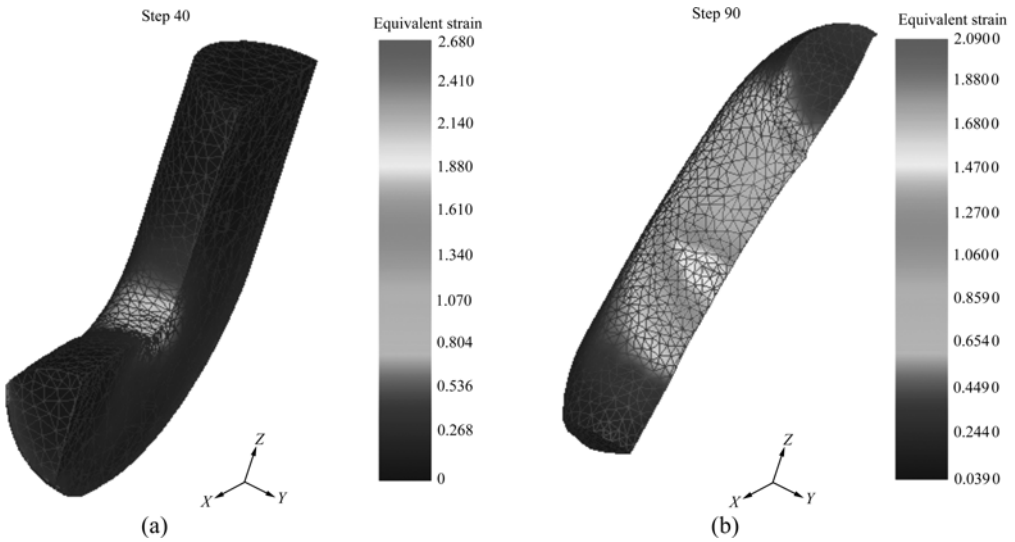

Fig.6 Distributions of equivalent strain with inner angle of 90˚ and inner round fillets: (a) Contours of equivalent stress of step 40; (b) Contours of equivalent strain of step 90

Table 4 Effective strains and deformation inhomogeneity index at extrusion step 90

ECAE die structure	ε_{max}	ε_{min}	ε_{ave}	C
Inner corner angle 90˚ without fillets	4.080	0.107	0.040 1	99.1
Inner corner angle 90˚ with fillets	3.727	0.390	0.055 6	60.0
Inner corner angle 120˚ without fillets	1.860	0.096	0.045 0	39.2
Inner corner angle 120˚ with fillets	1.620	0.070	0.040 0	38.8

angle of 90˚ and fillets at outer corner is the highest. We can draw a conclusion that raising the inner corner angle and machining fillets at outer corner would improve the forming homogeneity but reduce the cumulative strain simultaneously. To refine and homogenize simultaneously the microstructure of AZ31, a higher strain distribution and smaller inhomogeneity index are needed. So, the ECAE die with inner corner angle of 90˚ and fillets contributes to reach the aims.

3.3.2 Maximum strain during ECAE process

Fig.7 illustrates the maximum strain curves under different simulation conditions (illustrated in Fig.2) during the ECAE processes. The cumulated maximum strains calculated by Eq.(2) and simulation results are listed in Table 5.

From the simulation and theoretical calculation, we find that the cumulated maximum strains caused by the ECAE die with angle of 90˚ are larger than those of the die with angle of 120˚ with the fillets at outer corner manufactured and inner corner angle dropping. Increases of the maximum strains are due to the extrusion environment (temperature 300 ℃) and friction. The models in Fig.2(c) and Fig.2(d) are simulated under the same conditions. The maximum effective strain decreases sharply compared with the models in Fig.2(a) and Fig.2(b) with the same corner angles.

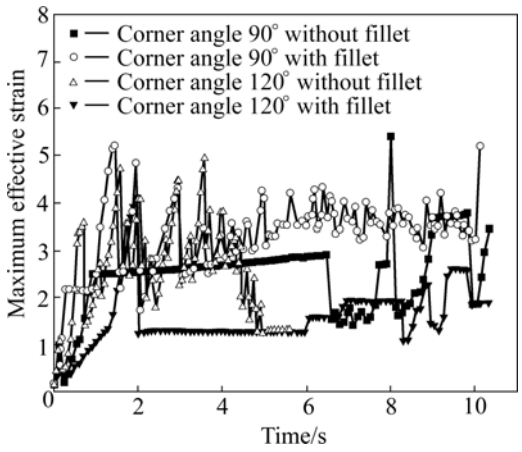

Fig.7 Maximum strain curves under different conditions

Table 5 Calculated and simulated cumulative maximum strains under different conditions during ECAE process

Condition	90˚		120˚	
	Calculation from Eq.(2)	Simulation results	Calculation from Eq.(2)	Simulation results
Without fillets at outer angle	3.17	5.45	2.30	5.0
With fillets at outer angle	2.93	5.20	0.92	4.1

$$\varepsilon = \frac{2\cot(\frac{\Phi}{2}+\frac{\Psi}{2})+\Psi\csc(\frac{\Phi}{2}+\frac{\Psi}{2})}{\sqrt{3}} \quad (3)$$

where Φ is the inner corner angle; Ψ is the outer corner

angle; ε is the strain.

The dynamic recrystallization is a function of strain, strain rate, temperature and initial grain size, which changes in time. The Avrami equation is used to describe the relation between the dynamically recrystallized fraction X and the effective strain. $\varepsilon_{0.5}$ is the strain for 50% recrystallization (mm/mm).

$$X = 1 - \exp[-\beta_d(\frac{\varepsilon - a_{10}\varepsilon_p}{\varepsilon_{0.5}})^{k_d}] \quad (4)$$

From Eq.(3), X increases with increasing the effective strain. It can be concluded that the dynamically recrystallized fraction caused by ECAE die with angle of 90˚ is much more than that induced by ECAE die with angle of 120˚ for the more strains caused by former die than the latter. In Refs.[19−20], AZ31 Mg alloy was prepared through two different equal channel angular pressing(ECAP) dies, in which the intersecting angles between channels were 90˚ and 120˚, respectively. Mechanical properties of the alloy after 12 passes of pressing in the 120˚ die are very close to those after 8 passes of pressing in the 90˚ die. That is to say, the strain per pass caused by 90˚ die is much larger that that by 120˚ die. After one pass ECAP, the alloy's microstructures were effectively refined by dynamic recrystallization(DRX). It could be found that one pass pressing brought about some tiny subgrains near some original coarse grains, and more fine grains appeared in the processing by the 90˚ die than that caused by 120˚ die. At the same time, the deformation inhomogeneity of microstructures caused by 120˚ die is larger than that caused by 90˚ die.

3.4 Curves of load and stroke

Fig.8 illustrates that the extrusion loads of simulations and experiments are various in the course of extrusions including the loads caused by corner angles of 90˚ and 120˚ die with or without fillets. The curves of force—stroke induced by dies with inner corner angle of 90˚ with fillets or not were measured by a pressure sensor and strokes from the above experiments. It is discovered that the simulation results are in agreement with the experimental results very well. In the initial strokes, extrusion forces are smaller; with the material extruded into the corner of bottom, the loads gradually climbed to the maximum values. Thereafter, the loads begin to drop slowly and fluctuate owing to the variation of frication caused by changing contact areas between the billet and wall of the bottom die. The maximum loads of the top die without fillets are 2 259, 3 040 N and the corresponding corner angles are 90˚ and 120˚, respectively. If the dies with fillets are used (shown in Fig.2(c), Fig.2(d)), the loads of top die go down compared with the corresponding angles without fillets. The required extrusion forces under different conditions are listed in Table 6. We can draw the conclusion that the fillets at the outer corner in ECAE die can reduce the requirement of extrusion forces for press.

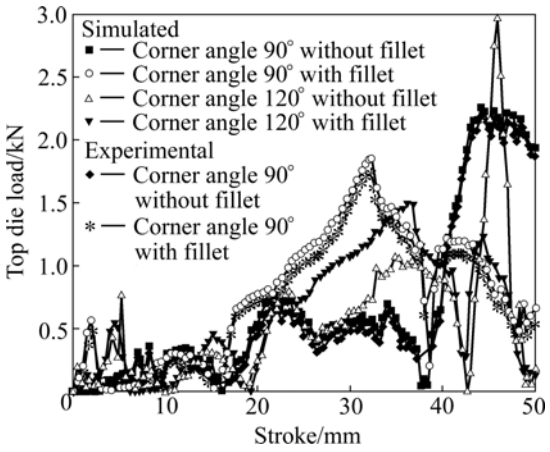

Fig.8 Curves of load—stroke under different conditions

Table 6 Required extrusion forces under different conditions (N)

Condition	90˚		120˚
	Simulation	Experiment	
Without fillets at outer corner	2 259	2 197	3 040
With fillets at outer corner	1 848	1 745	1 497

4 Conclusions

1) Numerical and physical modeling is helpful for understanding the deformation behavior of AZ31 magnesium alloy during ECAE. The importance of inner corner angle and outer corner fillets has been realized in this study.

2) It is found that the equivalent strains during the whole ECAE process are increased by comparing the 3D FEM simulation results with theoretical calculation because thermal and friction conditions are thought in simulations. Reasonable lubrication condition is important to plasticity deformation.

3) The deformation homogeneity caused by fillets of the outer corner is larger than that induced by the ECAE dies without outer corner fillets from the simulation and experimental results, because fillet at the inner channel surface junction where the two straight channels meet helps to process materials with high percentage of flow softening.

4) From the simulation and theoretical and literature results, the smaller inner corner angle can obtain the larger cumulative strains and bring about more tiny subgrains but decrease homogeneity simultaneously.

5) The loads of top die decline mainly with fillets of the bottom die manufactured.

6) The bottom die with outer corner fillets and inner corner angle of 90° is propitious to improve the plasticity and at the same time increases the deformation homogeneity of the rods to some extent.

References

[1] RAGHAVAN S. Computational simulation of the equi-channel angular extrusion process [J]. Scripta Mater, 2001, 44(1): 91−96.

[2] SUH J Y, KIM H S, PARK J W, CHANG J Y. Finite element analysis of material flow in equal channel angular pressing [J]. Scripta Mater, 2001, 44: 677−681.

[3] KIM J K, KIM W J. Analysis of deformation behavior in 3D during equal channel angular extrusion [J]. Journal of Materials Processing Technology, 2006, 176: 260−267.

[4] LANG Y, SHYONG L. Finite element analysis of strain conditions after equal channel angular extrusion [J]. Journal of Materials Processing Technology, 2003, 140: 583−587.

[5] LEE S C, HA S Y, KIM K T, HWANG S M, HUH L M, CHUNG H S. Finite element analysis for deformation behavior of an aluminum alloy composite containing SiC particles and porosities during ECAP [J]. Materials Science and Engineering A, 2004, 371: 306−312.

[6] ROSOCHOWSKI A, OLEJNIK L, RICHERT M. 3D-ECAP of square aluminum billets [J]. Advanced Methods in Material Forming, 2007, 10: 215−232.

[7] SUO Tao, LI Yu-long, DENG Qiong, LIU Yuan-yong. Optimal pressing route for continued equal channel angular pressing by finite element analysis [J]. Materials Science and Engineering A, 2007, 466: 166−171.

[8] SMOLYAKOV A A, VYACHESLAV P. Three-dimensional numerical simulations of multi-pass equal-channel angular pressing by a variation difference method and comparison with experiment [J]. Materials Science and Engineering A, 2008, 493: 148−159.

[9] LUIS PÉREZ C J, LURI R. Study of the ECAE process by the upper bound method considering the correct die design [J]. Mechanics of Materials, 2008, 40: 617−628.

[10] CHUNG S W, SOMEKAWA H, KINOSHITA T, KIM W, HIGASHI K. The non-uniform behavior during ECAE process by 3-D FVM simulation [J]. Scripta Mater, 2004, 50: 1079−1083.

[11] JIANG Hong, FAN Zhi-guo, XIE Chao-ying. 3D finite element simulation of deformation behavior of CP-Ti and working load during multi-pass equal channel angular extrusion [J]. Materials Science and Engineering A, 2007, 485: 409−414.

[12] HU Hong-jun, ZHANG Ding-fei, PAN Fu-sheng, YANG Ming-bo. Analysis of the cracks formation on surface of extruded magnesium rod based on numerical modeling and experimental verification [J]. Acta Metallurgica Sinica, 2009, 22: 353−364.

[13] ZHERNAKOV V S, LATYSH V V, ZHARIKOV A I, VALIEV R Z. The developing of nanostructure SPD Ti for structural use [J]. Scripta Mater, 2001, 44: 1771−1774.

[14] IWAHASHI Y, HORITA Z, NEMOTO M, LANGDON T G. The process of grain refinement in equal-channel angular pressing [J]. Acta Mater, 1998, 46: 3317−3331.

[15] MAENG D Y, KIM T S, LEE J H. Microstructure and strength of rapidly solidified and extruded Mg-Zn alloys [J]. Scripta Mater, 2000, 43: 385−389.

[16] SABATER M, GARCIA-ROMEU M L, CIURANA J. Input parameters determination for predicting ram speed and billet temperature for the first billet [J]. Key Engineering Materials, 2008, 367: 161−168

[17] LIU Chu-ming, LIU Zi-juan, ZHU Xiu-rong, ZHOU Hai-tao. Research and development progress of dynamic recrystallization in pure magnesium and its alloy [J]. The Chinese Journal of Nonferrous Metals, 2006, 16(1): 1−10.

[18] KIM I, KIM J, SHIN D H, LEE C S. Effects of equal channel angular pressing temperature on deformation structures of pure Ti [J]. Materials Science and Engineering A, 2003, 342: 302−310.

[19] SHIN D H, KIM B C, PARK K T, CHOO W Y. Microstructural changes in equal channel angular pressed low carbon steel by static annealing [J]. Acta Mater, 2000, 48: 3245−3252.

[20] LI S, BOURKE M A M, BEYERLEIN I J, ALEXANDER D J, CLAUSEN B. Finite element analysis of the plastic deformation zone and working load in equal channel angular extrusion [J]. Materials Science and Engineering A, 2004, 382(1): 217−236.

[21] YU Kun, LI Wen-xian, WANG R C. Researches, developments and applications of wrought magnesium alloys [J]. The Chinese Journal of Nonferrous Metals, 2003, 13(2): 277−288. (in Chinese)

[22] YU Kun, LI Wen-xian, WANG Ri-chu. Plastic deformation mechanism of magnesium alloys [J]. The Chinese Journal of Nonferrous Metals, 2005, 15(7): 1081−1086.

[23] CHEN Yong-jun, WANG Qiu-dong, LIN Ju-bao, ZHANG Lu-jun, ZHAI Chun-quan. Microstructure and mechanical properties of AZ31 Mg alloy processed by high ratio extrusion [J]. Transactions of Nonferrous Metals Society of China, 2006, 16(S3): 1875−1878.

[24] LI Yuan-yuan, LIU Ying, NGAI T L, ZHANG Da-tong, GUO Guo-wen, CHEN Wei-ping. Effects of die angle on microstructures and mechanical properties of AZ31 magnesium alloy processed by equal channel angular pressing [J]. Transactions of Nonferrous Metals Society of China, 2004, 14(1): 53−58.

[25] LI Yuan-yuan, ZHANG Da-tong, LIU Ying, LONG Yan, CHEN Wei-ping. Microstructure and tensile behavior of hot extruded AZ91 alloys at room temperature [J]. Journal of University of Science and Technology Beijing, 2002, 9(5): 352−355.

(Edited by YANG Hua)